Correction notice
Nature Phys. http://dx.doi.org/10.1038/nphys2294 (2012)

Experimental delayed-choice entanglement swapping
Xiao-song Ma, Stefan Zotter, Johannes Kofler, Rupert Ursin, Thomas Jennewein, Časlav Brukner and Anton Zeilinger

In the version of this Supplementary file originally posted online, the references in the section ‘Quantum random number generator’ were incorrect. The error has been corrected in this file 26 April 2012.

nature physics

SUPPLEMENTARY INFORMATION

DOI: 10.1038/NPHYS2294

Experimental delayed-choice entanglement swapping

Xiao-song Ma[1,2], Stefan Zotter[1], Johannes Kofler[1†], Rupert Ursin[1], Thomas Jennewein[1††], Časlav Brukner[1,3], and Anton Zeilinger[1,2,3]

[1] *Institute for Quantum Optics and Quantum Information (IQOQI), Austrian Academy of Sciences, Boltzmanngasse 3, A-1090 Vienna, Austria*

[2] *Vienna Center for Quantum Science and Technology (VCQ), Faculty of Physics, University of Vienna, Boltzmanngasse 5, A-1090 Vienna, Austria*

[3] *Faculty of Physics, University of Vienna, Boltzmanngasse 5, A-1090 Vienna, Austria*

† *Present Address: Max Planck Institute of Quantum Optics, Hans-Kopfermann-Str. 1, 85748 Garching/Munich, Germany*

†† *Present Address: Institute for Quantum Computing and Department of Physics and Astronomy, University of Waterloo, 200 University Ave W., Waterloo, ON, Canada N2L3G1*

The high-speed tunable bipartite state analyzer

We use a Mach-Zehnder interferometer (MZI) to realize the high-speed tunable bipartite state analyzer (BiSA). It consists of two 50:50 beam splitters, mirrors and most importantly two electro-optical modulators. The whole interferometer is built in a box enclosed with acoustic and thermal isolation materials in order to stabilize the phase passively. Additional to the passive stabilization, active phase stabilization is also employed as described in the main text. We define the phase of the interferometer to be zero when all the photons that entered from input b exited into b'' (Fig. 2), which is also the phase locking point of the interferometer. When the phase of the interferometer is $\pi/2$, the interferometer acts as a 50/50 beam splitter and performs Bell-state measurements. On the other hand, when the phase of the interferometer is 0, the interferometer acts as a 0/100 beam splitter, i.e. a fully reflective mirror, and performs separable-state measurements. Because of the short coherence time of the down-converted photon defined by the transmission bandwidth (1 nm) of the interference filter, it requires accurate path length adjustment of the two MZI arms. We minimize the path length difference by maximizing the single photon interference visibility when one input is blocked. Inside the tunable BiSA, two additional pairs of cross oriented BBO crystals (BBOs3 and BBOs4) are placed in each arm of the MZI in order to compensate the birefringence induced by the beam splitters.

As to electro optical modulators (EOM), we use Pockels Cells (PoC) consisting of two 4x4x10mm Rubidium

Titanyl Phosphate (RTP) crystals. We align the optical axes of the RTP crystals to 45° for both EOM1 and EOM2. Additionally, we place two eighth-wave plates (EWP) with their optical axes oriented parallel (in front of the EOM1) and orthogonal (in front of the EOM2) to the axis of the RTP crystals, respectively. Applying positive eighth-wave voltage (+EV) makes the EOM1 act as an additional eighth-wave plate. Given the fact that the optical axis of EWP1 is oriented parallel to that of RTP crystals, the overall effect is the one of a quarter-wave plate (QWP) at 45°. On the other hand, applying negative eighth-wave voltage (–EV) makes the EOM1 compensate the action of the EWP1, such that there is no overall effect. Since the optical axis of EWP2 is oriented orthogonal to that of the RTP crystal in EOM2, the overall effect is the one of a QWP at –45° by applying –EV and identity by applying +EV.

With opposite voltages on EOM1 and EOM2, we realize a $\pi/2$ phase change of the MZI (corresponding to Bell-state measurement) when EOM1 is applied with +EV and EOM2 with –EV, and no phase change (corresponding to separable state measurement) when EOM1 is applied with -EV and EOM2 with +EV.

A self-built field programmable gate array based logic samples the random bit sequence from the quantum random number generator (QRNG) and delivers the required pulse sequence for the PoC driver. Corresponding to the random bit value “1” (“0”) a phase change of the MZI of $\pi/2$ (0) is applied. A certain setting is not changed until the occurrence of an opposite trigger signal. Since our QRNG is balanced within the statistical uncertainties, +QV and –QV are applied equally often approximately. Therefore, the mean field in the PoC is zero which allows continuous operation of the PoC without damaging the crystals. For the fast and optimal operation of the PoC, a sampling frequency of 2 MHz is chosen. We set the on-time of both EOMs to be 299 ns, which guarantees that the choice is delayed by more than 14 ns. The duty cycle of our tunable BiSA is about 60%. For detailed information on this apparatus refer to Ref (*1*).

Using the bipartite state analyzer for Bell-state measurements

When used for a Bell-state measurement (BSM), our BiSA can project photons 2 and 3 onto two of the four Bell states, namely onto $|\Phi^+\rangle_{23} = (|HH\rangle_{23} + |VV\rangle_{23})/\sqrt{2}$ (both detectors in b’’ firing or both detectors in c’’ firing) and $|\Phi^-\rangle_{23} = (|HH\rangle_{23} - |VV\rangle_{23})/\sqrt{2}$ (one photon in b’’ and one in c’’ with the same polarization). When a separable-state measurement (SSM) is made, we look at coincidences between b’’ and c’’ with the same

polarization (as in the BSM case for $|\Phi^-\rangle_{23}$) and the resultant projected states are $|HH\rangle_{23}$ and $|VV\rangle_{23}$. Victor's detector coincidences with one horizontal and one vertical photon in spatial modes b'' and c'' indicate the states $|HV\rangle_{23}$ and $|VH\rangle_{23}$, which are always discarded because they are separable states independent of Victor's choice and measurement.

The working principle of the BSM can be explained in the following way: (a) If we detect a coincidence in the same spatial mode b''/c'' (as shown in Fig. 2 of the main text) but with different polarization in the $|H\rangle/|V\rangle$ basis, photons 2 and 3 are projected onto $|\Phi^+\rangle$ in spatial modes b and c (up to a global phase). This is because the state $|\Phi^+\rangle$ has the following evolution:

$$
\begin{aligned}
&|\Phi^+\rangle = (|HH\rangle_{\mathrm{bc}} + |VV\rangle_{\mathrm{bc}})/\sqrt{2} \\
&\xrightarrow{\text{BS 1}} i\,(|HH\rangle_{\mathrm{b'b'}} + |VV\rangle_{\mathrm{b'b'}} + |HH\rangle_{\mathrm{c'c'}} + |VV\rangle_{\mathrm{c'c'}}))/(2\sqrt{2}) \\
&\xrightarrow{\text{EWPs \& EOMs}} (|RR\rangle_{\mathrm{b'b'}} - |LL\rangle_{\mathrm{b'b'}} + |LL\rangle_{\mathrm{c'c'}} - |RR\rangle_{\mathrm{c'c'}})/(2\sqrt{2}) \\
&\xrightarrow{\text{BS 2}} -i(|HV\rangle_{\mathrm{b''b''}} - |HV\rangle_{\mathrm{c''c''}})/\sqrt{2};
\end{aligned}
$$

(b) If we detect a coincidence in different spatial modes b'' and c'' but with same polarization in the $|H\rangle/|V\rangle$ basis, photons 2 and 3 are projected onto $|\Phi^-\rangle$ in spatial modes b and c (up to a global phase). This is because the state $|\Phi^-\rangle$ has the following evolution:

$$
\begin{aligned}
&|\Phi^-\rangle = (|HH\rangle_{\mathrm{bc}} - |VV\rangle_{\mathrm{bc}})/\sqrt{2} \\
&\xrightarrow{\text{BS 1}} i\,(|HH\rangle_{\mathrm{b'b'}} - |VV\rangle_{\mathrm{b'b'}} + |HH\rangle_{\mathrm{c'c'}} - |VV\rangle_{\mathrm{c'c'}}))/(2\sqrt{2}) \\
&\xrightarrow{\text{EWPs \& EOMs}} (|RR\rangle_{\mathrm{b'b'}} + |LL\rangle_{\mathrm{b'b'}} + |LL\rangle_{\mathrm{c'c'}} + |RR\rangle_{\mathrm{c'c'}})/(2\sqrt{2}) \\
&\xrightarrow{\text{BS 2}} -i(|HH\rangle_{\mathrm{b''c''}} - |VV\rangle_{\mathrm{b''c''}})/\sqrt{2}
\end{aligned}
$$

According to the calculations above, for a specific result of Victor's Bell-state measurement in our experiment, photons 2&3 are projected onto the entangled state $|\Phi^+\rangle_{23} = (|HH\rangle_{23} + |VV\rangle_{23})/\sqrt{2}$ with the tunable BiSA. This projects photons 1 and 4 onto the state $|\Phi^+\rangle_{14}$, as shown in Eq. (2). Note that although it is possible to choose, via the QRNG, whether to project the quantum state of two photons onto an entangled or a separable

state, it is not possible to choose onto which particular state. The outcome of the BSM (SSM) is random and hence one cannot have prior knowledge of whether one obtains $|\Phi^-\rangle_{23}$ or $|\Phi^+\rangle_{23}$ ($|HH\rangle_{23}$ or $|VV\rangle_{23}$) for each individual run. The experimental results of the correlation functions of photons 1 and 4 in the $|H\rangle/|V\rangle$, $|R\rangle/|L\rangle$ and $|+\rangle/|-\rangle$ bases are 0.589 ± 0.078, –0.561 ± 0.078, 0.59 ± 0.072, respectively. A state fidelity $F\left(\hat{\rho}_{\mathrm{exp}}, |\Phi^+\rangle_{14}\right)_{\mathrm{BSM}}$ of 0.685 ± 0.033 is obtained and the entanglement witness value $W\left(\hat{\rho}_{\mathrm{exp}}, |\Phi^+\rangle_{14}\right)_{\mathrm{BSM}}$ is –0.185 ± 0.033. Therefore, entanglement between photons 1 and 4 is verified.

When Victor performs a BSM, photons 1 and 4 are only entangled if there exists the information necessary for Victor to specify into which subensembles the data are to be sorted. In our case the subensembles correspond to $|\Phi^-\rangle_{23}$ or $|\Phi^+\rangle_{23}$. Without the ability for this specification, he would have to assign a mixture of these two Bell states to his output state which is separable, and thus he could not correctly sort Alice's and Bob's data into subensembles. This is confirmed by evaluating the experimental data obtained in a BSM but without discriminating between $|\Phi^-\rangle_{23}$ and $|\Phi^+\rangle_{23}$. Then there exists a correlation only in the $|H\rangle/|V\rangle$ basis (0.55 ± 0.06) and no correlations in the $|+\rangle/|-\rangle$ (0.02 ± 0.05) and $|R\rangle/|L\rangle$ (0.01 ± 0.05) bases, similar to the situation when Victor performs a separable-state measurement.

Quantum random number generator

Refs. [6, 21] of the main text describe the details of the working principle of our quantum random number generator (QRNG). A weak light beam from a light emitting diode splits on a balanced optical beam splitter. Quantum theory predicts that each individual photon, which is generated from the source and travels through the beam splitter, has the same probability for both output arms of the beam splitter. Photon multipliers (PM) are used to detect the photons on each output, labeled by '0' and '1'. When PM '0' fires, the bit value is set to 0. It remains 0 until PM '1' detects one photon, which flips the bit value to 1. Thus, the bit sequence produced by the QRNG is truly random according to quantum theory.

Four-fold count rate and error estimation

Photons 1 and 4 are filtered with two interference filters of 3 nm FWHM bandwidth, and photons 2 and 3 are filtered with 1 nm IFs. We have detected the 2-fold count rate directly (without tunable BiSA) of about 20 kHz,

and about 4.9 Hz 4-fold count rate with a pump power of 700 mW. There are two reasons for the relatively low detected 4-fold coincidence counts. The first one is to avoid the higher order emissions from spontaneous parametric down conversion (SPDC). Therefore, we could not pump the crystal with too high pump power[2]. In this experiment, we just used 700 mW, half of the maximal pump power. The second reason is the loss on various optical components and the duty cycle of the EOMs. We lost 79% of the photons on each individual input of the tunable BiSA (including the 104 m single mode fiber), which results in 4.4% photons left. The probabilistic nature of the Bell-state projection with linear optics decreases the success probability to 1/4. The random choices to either perform BSM or SSM determined by the QRNG gives an additional trivial reduction of 1/2 for each individual measurement. As explained above, the duty cycle of the EOMs are not unity, which reduces the count rate to 0.6. Including all of these losses, we are left with the fraction 0.0033 of the initial 4.9 Hz for each individual measurement. Therefore, the detected four-fold rate is about 0.016 Hz, as stated in the captions of Fig. 2 in the letter.

The limited state fidelities are mainly due to the higher order emissions from SPDC, although we have deliberately reduced the UV pump power. We have developed a numerical model to calculate the expected results. This model is based on the interaction Hamiltonian of SPDC. Given an interaction strength (or squeezing parameter) of the pump and nonlinear crystal, which can be measured experimentally, one can expand the Hamiltonian into a Taylor series. From this expansion, we can estimate the noise from the higher order emission. We utilized a quantum optics toolbox in Matlab[3], based on a matrix representation of quantum states with up to three photons per mode. With this model, it is straightforward to reproduce the count rates and visibilities of our system. In the model the detection efficiency is determined by the specifications of the single photon detectors and the coupling efficiency is measured and derived from the ratio of the 2-fold coincidence counts and single counts. From this calculation, the expected correlation function of photons 1 and 4 is about 0.674.

The other reason which limits the state fidelities is the group velocity mismatch of pump photons and the down converted photons in the type-II phase matching of BBO crystal[4]. A rigorous model for calculating that can be found in refs. (*5,6*). The expected correlation function of photons 1 and 4 decreases to 0.964.

We are also limited by experimental imperfections. For instance, the performance of the tunable BiSA, which is

limited by the visibility of the MZI (0.95) and the switching fidelity (0.99), is about 0.94. The polarization alignment in the fibers, which quantifies the transmission fidelity of the photon in the fibers, is about 0.99.

The overall expected correlation function of photons 1 and 4 is the product of all above listed values and equals to 0.605, which is in good agreement with our measured value.

Experimental fulfilling of the delayed-choice condition

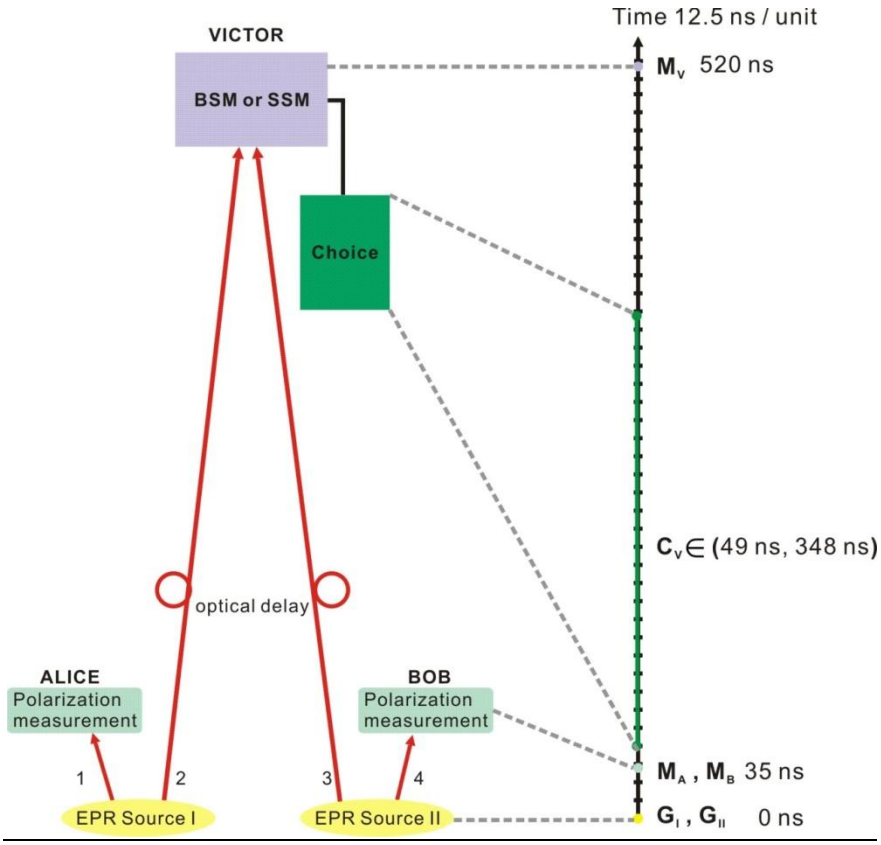

Figure 1: Time diagram of our delayed-choice entanglment swapping experiment. Two polarization entangled photon pairs (1&2 and 3&4) are generated from Einstein-Podolsky-Rosen (EPR) sources I and II (events $\mathbf{G_I}$ and $\mathbf{G_{II}}$) at 0 ns. The polarizations of photons 1 and 4 are measured by Alice (event $\mathbf{M_A}$) and Bob (event $\mathbf{M_B}$) 35 ns later. The other two photons (photons 2 and 3) are delayed and then sent to Victor who can choose (event $\mathbf{C_V}$) to swap the entanglement or not by performing a Bell-state measurement (BSM) or a separable-state measurement (SSM) on photons 2 and 3 (event $\mathbf{M_V}$). Victor's choice and measurement are made after Alice and Bob's polarization measurements. Remarkably, whether the earlier registered results of photons 1 and 4 indicate the existence of entanglement between photons 1 and 4 depends on the later choice of Victor.

The experimental scheme and the time diagram of the relevant events is shown in Fig. 1. We assigned that the generation of photons 1 and 2 (event $\mathbf{G_I}$) happened at 0 ns, as the origin of the diagram. The generation of photons 3 and 4 (event $\mathbf{G_{II}}$) happened 1.6 ns later. At 35 ns, the measurements of Alice and Bob (events $\mathbf{M_A}$ and $\mathbf{M_B}$) occurred. The choice of Victor (event $\mathbf{C_V}$) was made by the QRNG in the time interval ranging from 49 ns to 348 ns and sent to the tunable BiSA. Due to the fibre delay of photons 2 and 3, at 520 ns Victor performed the bipartite state measurement (event $\mathbf{M_V}$) according to the bit value of his choice. Note that our definition of the choice event is very conservative. This is because in addition to the fixed amount of the electrical delay of the EOMs' driver (45 ns), QRNG (75 ns) and connecting cables (20 ns), we also included 3 times the QRNG autocorrelation time ($3 \cdot 10.7$ ns $\approx$ 32 ns) and the on-time of the EOMs (299 ns). This on-time gave the time of event $\mathbf{C_V}$ a lower bound of 49 ns and an upper bound of 348 ns. As shown in Fig. 1, it is clear to see for each successful run (a 4-fold coincidence count) that not only event $\mathbf{M_V}$ happened 485 ns later than events $\mathbf{M_A}$ and $\mathbf{M_B}$, but also event $\mathbf{C_V}$ happened 14 ns to 313 ns later than events $\mathbf{M_A}$ and $\mathbf{M_B}$ even in this conservative consideration. Therefore, with this configuration we unambiguously fulfilled the delayed-choice condition. Note that the main uncertainty of our experiment in time for measurements is the detector jitter, which is about 800 ps.

References:

1. X.-S. Ma *et al.,* A high-speed tunable beam splitter for feed-forward photonic quantum information processing. *Opt. Express*, **19**, 22723-22730 (2011).
2. A. Lamas-Linares, J. C. Howell, D. Bouwmeester, Stimulated emission of polarization-entangled photons. *Nature*, **412**, 887-890 (2001).
3. S.-M. Tan, A computational toolbox for quantum and atomic optics. *J. Opt. B: Quantum Semiclass. Opt.* **1**, 424 (1999).
4. P. Mosley *et al.*, Heralded Generation of Ultrafast Single Photons in Pure Quantum States. *Phys. Rev. Lett.* **100**, 133601 (2008).
5. T. Jennewein, R. Ursin, M. Aspelmeyer, A. Zeilinger, Performing high-quality multi-photon experiments with parametric down-conversion. *J. Phys. B: At. Mol. Opt. Phys.* **42**, 114008 (2009).
6. R. Kaltenbaek, Entanglement swapping and quantum interference with independent sources. Ph.D. thesis, University of Vienna (2008).